17th World Conference on Nondestructive Testing, 25-28 Oct 2008, Shanghai, China

Non-destructive Characterization of Pearlite Spheroidisation by Magnetic Barkhausen Noise Method

C. Hakan GÜR, Kemal DAVUT

Metallurgical and Materials Eng. Dept. Middle East Technical Univ. Ankara, Turkey
Welding Technology and NDT Research/Application Center, METU-Ankara, Turkey
chgur@metu.edu.tr http://www.mete.metu.edu.tr http://www.wtndt.metu.edu.tr

Abstract

The aim of this study is to investigate the effects of spheroidising heat treatment on steels by Magnetic Barkhausen Noise (MBN) method. Various series of specimens consisting of either lamellar pearlite or partially/completely spheroidised carbides were produced from SAE 1060 steel by appropriate heat treatments. Samples were characterized by metallographic examinations and MBN measurements. The results showed that the evolution of microstructure as a result of spheroidisation, from coarse lamellar carbides to uniformly dispersed spherical carbides in ferrite matrix, is reflected as higher Barkhausen activity due to less effective pinning of domain walls.

Keywords: Spheroidising, Microstructure, Steel, Magnetic Barkhausen Noise

1. Introduction

Spheroidisation is a commercial heat treatment for medium and high carbon steels to improve formability and machinability, or to develop an appropriate microstructure for subsequent hardening treatments. These microstructures will form in any prior microstructure by heating at sufficiently high temperatures for sufficiently long periods to permit the diffusion dependent development of spherical cementite particles. Magnetic Barkhausen noise (MBN) measurement might be a good candidate for non-destructive monitoring the degree of spheroidisation in steels.

When a variable external field influences a ferromagnetic material, irreversible jumps of walls cause the formation of Barkhausen noise. High resolution examination of hysteresis cycles of ferromagnetic materials reveals discontinuous flux changes due to irreversible domain wall motion. Microstructural features such as dislocations, inclusions and grain boundaries, pin the domain walls. When the strength of externally applied magnetic field reaches the critical level, motion of the domain wall continues by Barkhausen jumps. These jumps can be detected as voltage pulses induced in a pick-up coil positioned close to the surface. These signals are processed using a software for characterization of the samples [1-2].

The size and distribution of the carbide particles strongly affect the Barkhausen signals. The MBN profiles of quenched and tempered 0.2%C steels change from single peak to double peak after tempering about 15-100 h [3]. During spheroidisation of pearlitic steels a decrease in the peak ratio of magneto acoustic emission profile and the formation of a second

peak in the magnetic Barkhausen noise profile were observed [4]. In ferritic – pearlitic steels it was found that increasing ferrite content decreases Barkhausen activity in low-field region and causes formation of outer peaks in the MBN profiles [5-8]. This study aims to detect the stages of spheroidising of steels by MBN method. By applying spheroidisation treatment on SAE 1060 specimens, a series of samples consisting of either lamellar pearlite or partially/completely spheroidised carbides in ferritic matrix were obtained.

2. Experimental

Samples having 8 mm thickness were cut from cold drawn SAE 1060 bar whose chemical composition is given in Table 1. Machining operations were done before heat treatments in order to avoid creation of surface residual stresses. All specimens were annealed at 800^{o}C for 1 hour. One specimen was left in annealed condition to compare the results with a pearlitic structure. Other specimens were further treated at 700^{o}C for 24, 48 and 72 hours followed by furnace cooling.

Table 1. Chemical composition (wt. %) of SAE 1060

C	Cr	Mo	Mn	Si	P	S	Fe
0.56	0.27	0.01	0.77	0.23	< 0.003	0.047	Bal.

For metallographic investigation, the samples were finely ground, and polished with alumina, then etched by picral solution. Quantitative measurements of degree of spheroidization, aspect ratio, size and distribution of cementite particles were done by Clemex Image Analysis software from the SEM micrographs. The criterion of 5:1 aspect ratio or less for spheroidization was used to measure the degree of spheroidisation. The degree of spheroidisation was calculated as volume percent of spheroidised particles.

MBN measurements were performed using a commercial system (μscan 500-2). During measurements a sinusoidal cyclic magnetic field with an excitation frequency of 20 Hz was induced in a small volume of the specimen via a ferrite core C-coil. The Barkhausen signals were filtered (0.1-300 kHz), and analyzed. The peak magnetizing voltage was 8V and sampling frequency was 2 MHz. During the analyses 30 bursts in average were used to obtain Barkhausen parameters for each specimen where each burst represents one half of the magnetization cycle.

3. Results and discussion

Figure 1 shows the SEM micrographs of the specimens. Fig. 1a shows the microstructure of the starting sample consisting of proeutectoid ferrite (about 25%) and alternating lamellae of ferrite and cementite that made up the pearlite (75%). The spacing variations of cementite lamellae in different areas may be partly due to differences in the angles that the lamellae make with the plane of polish, and partly due to the fact that the pearlite may have formed over a range of temperatures. The transformation of austenite into proeutectic ferrite occurs preferentially at grain boundaries and growth continues until a continuous layer is formed along the boundary. Figure 1.b shows the microstructure of the almost completely spheroidised specimen that was heated for 72 h at 700^{o}C. The average diameter of cementite

particles increases with time, due to disappearance of the smaller particles and growth of larger ones. To reduce the interfacial energy, cementite lamellae break up into smaller particles that eventually assume spherical shapes. Once the lamellae have broken up, the small spherical particles dissolve, and larger particles grow, again driven by the reduction in interfacial energy [9].

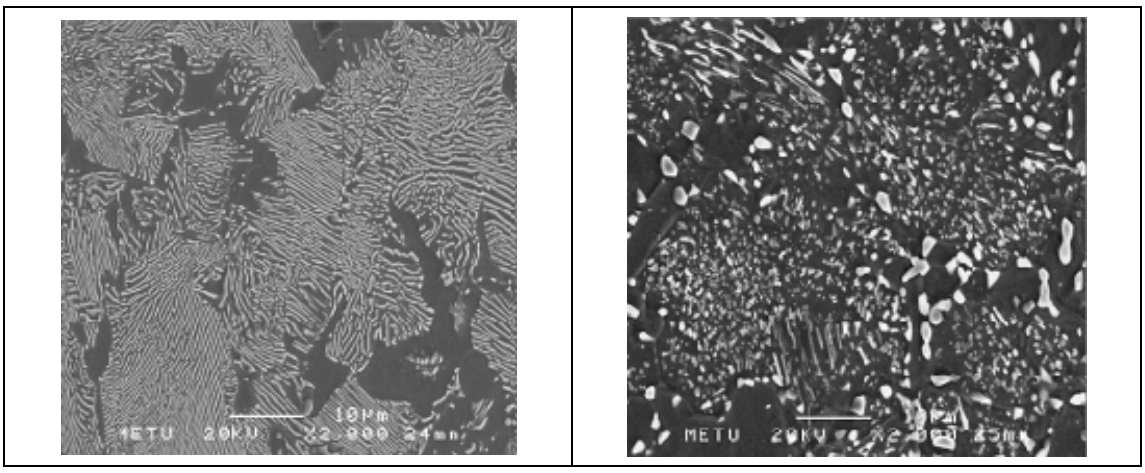

a **b**

Figure 1. Microstructures of the specimens

Figure 2 shows the curves for MBN signal versus applied field strength (MBN fingerprint). As MBN is symmetrical with respect to zero magnetic field, only the curves for the increasing applied magnetic field were plotted. The peak positions were obtained by fitting a parabola to the 15% of the top of the MBN curve. The ferritic-pearlitic specimen has the weakest MBN peak positioned at the highest field. As spheroidising duration increases, the amplitude of the peaks increases and peak position shifts to lower magnetic field strength. Under the effect of an alternating magnetic field, a representative magnetic hysteresis loop was induced in the small volume measured due to the energy loss with the irreversible process of magnetization. The MBN signal is generated due to sudden changes in magnetization and the irreversible motion of 180^{o} domain walls is the main contribution [10]. Consequently, the domain wall density and the mean free path of the domain wall displacement will decide the MBN peak height.

The nature of pinning sites for domain walls in the samples is mainly determined by cementite lamellae in pearlite grains. During MBN measurements, after the sample has been magnetized, reversal of magnetization is preceded by the sudden nucleation of domain walls, or by releasing domain walls trapped onto the pinning sites, such as cementite lamellae. The large interfacial area of cementite lamellae, which in turn increases volume fraction of pinning sites, definitely increases the energy loss during the magnetization process. Also the average distance between pinning obstacles should be determined by the inter-lamellar spacing of the pearlite which in turn restricts the movement of domain walls. Ferritic-pearlitic sample has the weakest MBN peak positioned at the highest field linked with higher coercivity. In this sample domain walls tend to be pinned at the cementite lamellae, and the unpinning of domain walls occurs at a higher reverse field.

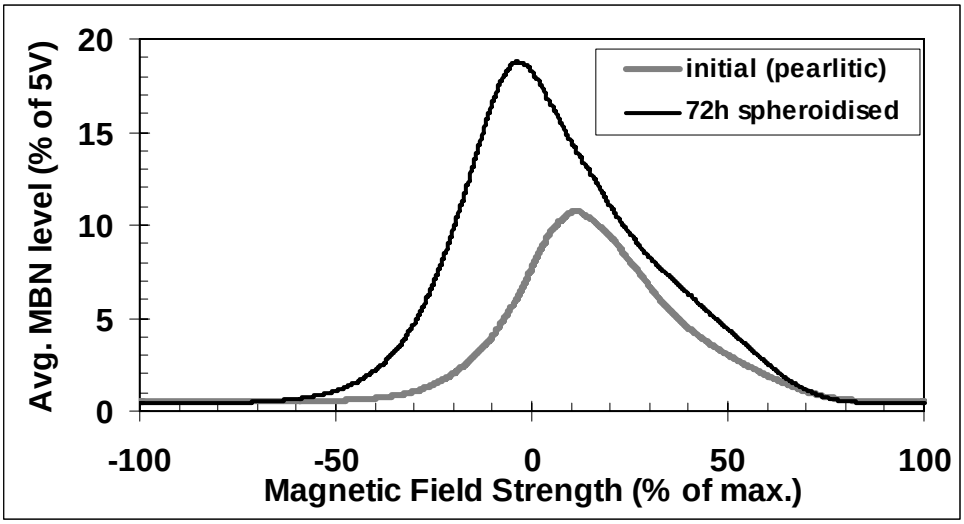

Figure 2. MBN profiles of the specimens

Better surface to volume ratio of spheroidised cementite, decreases the effective surface area of pinning sites. In addition, average distance between pinning sites increases allowing domain walls to move more freely. A weaker field is enough for the reversal of magnetization because of easier domain wall displacements. As spheroidising time increases cementite lamellae are completely disappeared, and almost all of the cementite are spheroidised. These morphological changes result in a drastic increase in the MBN peak and a clear shift to lower magnetic field in the peak position by reducing the resistance to the movement of domains.

The raw magnetic noise data consists of a series of voltage pulses and associated magnetic field values. The change of microstructure, which is quantified by the volume percent of spheroidal cementite particles, can be correlated to the MBN parameters (Fig. 3). The pearlitic specimen has the lowest RMS value. As spheroidisation continues, RMS value increases. Pinned domain walls due to large surface area of cementite lamellae cause lower RMS values in the pearlitic specimen. For longer spheroidization periods RMS value increases due to enhancement of domain wall displacement.

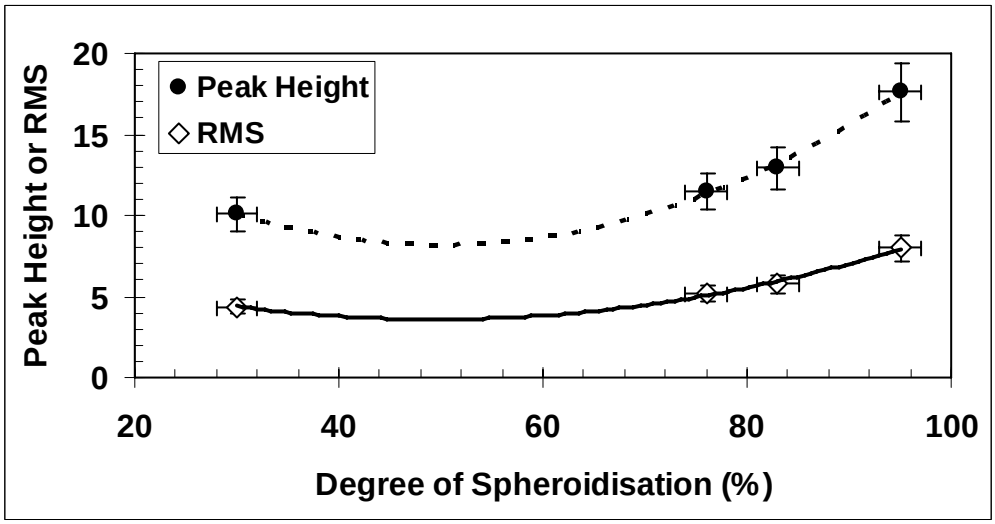

Figure 3. Degree of spheroidisation and MBN parameter correlation

The frequency spectrum shows the intensity of the noise given by the square voltage (V^2) as a function of the frequency. The frequency spectrum is calculated in the given analyzing frequency range (0,1 – 1000 kHz) using "Fast Fourier Transform" algorithm. The intensity of low frequency MBN signals increases as the spheroidisation continues (Fig. 4). Since frequency is inversely proportional to time, low frequency content of MBN signal indicates larger domain wall displacements if the average wall velocity is constant. In the annealed specimen domain wall displacements are short due to smaller the interlamellar spacing of pearlite, which determines the free path of domain wall displacement. As spheroidisation continues the cemetite lamellae break up into spherical carbides and the resistance to wall motion decreases which in turn causes an increase in the low frequency content of MBN. Partial spheroidisation causes a slight increase in the intensities due to presence of broken-up cementite plates which can still be effective pinning sites. The complete spherodisation of structure produces spherical cementite particles whose resistance to wall motion is quite low and causes an abrupt increase in the intensity of low frequency MBN signals. The coarsening of the cementite particles formed during early stages of spheroidisation has also an additional effect on MBN behaviour of the completely spherodised specimen.

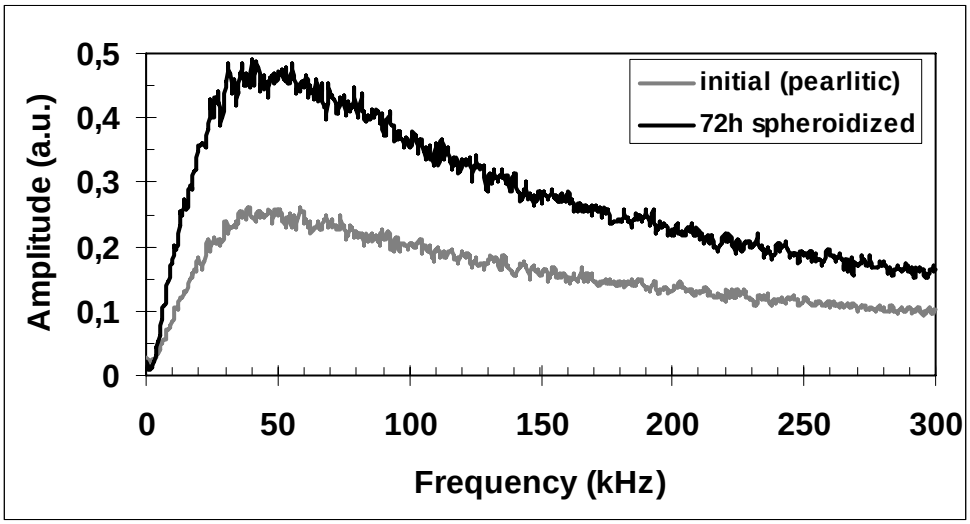

Figure 4. Frequency spectrums of the specimens

4. Conclusions

During spheroidisation of SAE 1060 steel specimens, cementite morphology changes from lamellar to spheroidal which is driven by the reduction in surface area. The large surface area of cementite lamellae in the pearlitic sample causes effective pinning of domain walls. Thus, the pearlitic sample has the weakest MBN peak positioned at the highest peak strength. As the degree of spheroidisation increases, the average distance between pinning cementite particles increases and the surface area of pinning sites decreases. Thus, Barkhausen activity increases, i.e., MBN peak gets higher and shifts to lower applied field strengths. Beside, magnetization reversal occurs at lower applied magnetic fields since domain walls can move more freely. A good correlation between hardness and MBN peak height or RMS of the spheroidised samples has also been observed. It has been concluded that MBN method can be utilized efficiently and effectively for characterisation of the spheroidised steel components.

Acknowledgements: Authors are thankful to Dr. Ibrahim Cam and METU-Central Laboratory for the MBN measurements; to Göksu Gürer and Sadık Bayramoglu for their help for the heat treatments.

References

1. Montalenti,G. Barkhausen noise in ferromagnetic materials. Zeitschrift für angewandte Physik, 1970(28), 295-300
2. Gaunt,P. Magnetic coercivity. Journal of Physics, 1987(65), 1194-1199
3. Moorthy,V., Vaidyanathan,S., Jayakumar,T. and Raj,B. Microstructural characterization of quenched and tempered 0.2% carbon steel using magnetic Barkhausen noise analysis. Journal of Magnetism and Magnetic Materials, 1997(171), 179-189
4. Lo,C.C.H., Jakubovics,J.P., Scruby,C.B. Non-destructive evaluation of spheroidised steel using magnetoacoustic and Barkhausen emission. IEEE Transactions on Magnetics, 1997(33), 4035-4037
5. Lo, C.C.H. and Scruby, C.B. Study of magnetization processes and the generation of magnetoacoustic and Barkhausen emissions in ferritic/pearlitic steel. Journal of Applied Physics, 1999(85), 5193-5195
6. Gür C.H, Özer M., Erdoğan M. Investigation of the variations in microstructure and mechanical properties of dual matrix ductile iron by magnetic Barkhausen noise analysis, Research in ND Evaluation, 19 (2008) 44-60
7. Davut K., Gür C.H. Monitoring the microstructural changes during tempering of quenched SAE 5140 steel by magnetic Barkhausen noise, J Nondestructive Evaluation, 26 (2007) 107-113
8. Kaplan M., Gür C.H., Erdoğan M. Characterization of dual-phase steels using magnetic Barkhausen noise technique, J Nondestructive Evaluation, 26 (2007) 79-87
9. Krauss, G. Steels: Heat Treatment and Processing Principles. (ASM International, Materials Park, Ohio, 1989)
10. Ranjan, R. Microstructural characterization of ferromagnetic materials using magnetic NDE tecniques. Materials Science and Engineering, p. 115 (Iowa State University, Ames, Iowa, 1987)